Proceedings of the Combustion Institute 40 (2024) 105667

Contents lists available at ScienceDirect

Proceedings of the Combustion Institute

journal homepage: www.elsevier.com/locate/proci

Predicting the autoignition behaviour of tailorable advanced biofuel blends using automatically generated mechanisms

Christian Michelbach [a,*], Khaiyom Hakimov [b], Aamir Farooq [b], Alison S. Tomlin [a]

[a] School of Chemical and Process Engineering, University of Leeds, Leeds LS2 9JT, United Kingdom
[b] Physical Sciences and Engineering Division, King Abdullah University of Science and Technology (KAUST), Thuwal 23955, Saudi Arabia

ARTICLE INFO

Keywords:
Automatic mechanism generation
Autoignition
Alcoholysis
Rapid compression machine
Advanced biofuels

ABSTRACT

Emerging processes such as biomass alcoholysis have the potential to provide tailorable, advanced biofuels to replace conventional fossil fuels. Knowledge of the engine-relevant behaviour for such fuels is evolving but is currently limited. Simulation tools may assist in the exploration of this behaviour but are reliant on the availability of robust, detailed kinetic mechanisms to produce accurate predictions. Automatic mechanism generation (AMG) techniques may be applied to facilitate the production of such mechanisms, as long as the utilised databases contain high-quality kinetic and thermochemical information of relevance to the functional groups of interest. To model the combustion characteristics of complex fuel blends, Reaction Mechanism Generator (RMG) is applied in this work to produce detailed ethyl (ethyl levulinate, diethyl ether, ethanol) and butyl (n-butyl levulinate, di-n-butyl ether, n-butanol) kinetic mechanisms. The predictive capabilities of these mechanisms are evaluated against a combination of literature data for individual components and new experimental measurements of ethyl and butyl blends. Stoichiometric blend ignition delay times are measured in a rapid compression machine at a compressed pressure of 20 bar and compressed temperatures of 645–960 K. The investigated blends are formulated to achieve a desired research octane number (blends ELV1 and BLV1) or to match physical property limits of diesel fuels (blends ELV2 and BLV2). Ethyl blend measurements show clear examples of complex low temperature oxidation behaviour, but this is not observable in the butyl cases, as the high boiling point of butyl levulinate necessitates the use of significant dilution in ignition delay experiments. The generated models show a high degree of accuracy when compared to measurements at thermodynamic conditions of relevance to engine technologies. The blending behaviour shown by the experimental measurements is also well predicted. This work highlights the importance of database additions/modifications based on low uncertainty, high quality, literature data when using AMG methods.

1. Introduction

Global energy demand is predicted to grow significantly, due largely to a rise in global population and the increasing demands of developing regions for transportation and goods haulage [1]. These sectors are heavily reliant on crude oil based fuels, raising climate concerns which must be addressed rapidly. In Europe, the Renewable Energy Directive II (RED II) requires that member states meet legally binding renewable energy targets, including a minimum of 14 % renewables for all road and rail transport by 2030 [2]. Furthermore, this directive limits the contribution of unsustainable first-generation biofuels to this target, while encouraging the use of advanced biofuels. Emerging technologies, such as biomass alcoholysis, could provide economically viable, tailorable, advanced biofuel blends [3].

The alcoholysis of biomass produces three primary products: an alkyl levulinate, a dialkyl ether, and an alcohol. Their ratios can be tailored by altering process parameters, allowing for the production of bespoke fuel blends to meet specific combustion requirements [4]. Ethyl and butyl alcoholysis processes are currently the most feasible for advanced biofuel production, as biogenic sources for ethanol and butanol are functional and well understood [5,6]. Tailoring fuels requires a comprehensive understanding of the combustion behaviour for each independent component and their blends.

Howard et al. [4] investigated the ignition behaviour of various blends of ethyl levulinate (EL), ethanol, and diethyl ether (DEE), using an ignition quality tester (IQT) and rapid compression machine (RCM).

* Corresponding author.
E-mail address: c.michelbach@leeds.ac.uk (C. Michelbach).

https://doi.org/10.1016/j.proci.2024.105667
Received 3 December 2023; Accepted 10 July 2024
Available online 31 July 2024

The work described blending regimes for Derived Cetane Number (DCN) and Research Octane Number (RON), and identified a blending ratio for a RON 95, MON 88.3, "ethanolic gasoline" (EG). Upon comparison to a FACE-F gasoline of almost identical octane ratings, they found that their EG produced similar reactivity at a compressed pressure (P_c) of 20 bar, including the presence of a negative temperature coefficient (NTC) region. However, this behaviour was muted for the EG blend, providing a shallower NTC profile. This was attributed to the increased role of HO_2 related chain termination, but uncertainty in DCN determination and the DCN to RON relation were potential sources of error [4,7]. Galletti et al. [8] reported on the performance and emissions impacts of blending diesel with ternary mixtures of n-butyl levulinate (nBL), n-butanol, and di-n-butyl ether (DNBE). Biofuel fractions of up to 20 % were shown to produce reductions in CO and particulate emissions, with no significant changes to engine power or fuel efficiency [8]. Despite these promising results, ignition studies of butyl levulinate and butyl blends are entirely absent from the literature, while studies of ethyl levulinate and ethyl blends are scarce.

Characterising the blending space for ethyl and butyl systems experimentally would be extremely costly. However, computational modelling provides an opportunity to predict combustion behaviour relatively cheaply and quickly. This requires a robust, detailed chemical kinetic mechanism. The large, detailed mechanisms typical of advanced biofuels may contain hundreds of species and thousands of reactions. Creating such mechanisms by hand is often tedious, prone to human error, and requires extensive expert knowledge of reaction pathways. Automatic Mechanism Generation (AMG) methods can limit the likelihood of human error by automating processes and embedding expert understanding through the algorithmic generalisation of thermochemical and kinetic data, instead of relying on complex machine learning tools [9]. AMG tools have been commonly applied successfully in the generation of mechanisms which describe the oxidation of non-oxygenated, non-aromatic hydrocarbons [10], as well as individual oxygenated species [11,12]. The emergence of advanced biofuels, which may contain a variety of complex structures and oxygenated functional groups, introduces new challenges for AMG. However, previous work [12] has shown that such tools can overcome these challenges (when appropriate training data are incorporated) and are capable of producing mechanisms which outperform their traditionally constructed counterparts across a range of key combustion targets.

This study uses AMG to produce mechanisms for ethyl and butyl biofuel blends. Their predictive capabilities are firstly evaluated against literature data of pure components. The autoignition behaviour of select ethyl and butyl blends is then predicted and evaluated against new measurements.

2. Methodology

2.1. Mechanism generation

Reaction mechanisms for each component were produced using Reaction Mechanism Generator (RMG) [13], following the AMG methodology proposed in the authors' previous case study of DEE [12]. Individual mechanisms were then combined to produce blend mechanisms for ethyl and butyl cases. RMG is one of the most frequently utilised AMG packages, commonly applied in the construction of detailed kinetic models, as well as the estimation of thermochemical properties [14]. Full details of RMG are given in the literature [13], though the general methodology is briefly summarised here. To initialise mechanism generation, RMG must first be provided with reactor conditions, species concentrations, termination criteria, and model tolerances. Initial species are then reacted together in the model core using a predefined set of reaction templates to form a model edge of product species. The rates for these reactions are estimated using a built-in database of rate rules and training data. It is therefore imperative that this underlying database contains accurate training data. All possible elementary reactions are considered, while a rate-based algorithm determines whether to include each edge species (and associated reactions) in the model core [15]. RMG generated pressure dependent reaction networks are explored using the modified strong collision (MSC) method, which has a much smaller computational cost than full master equation models, usually providing a good degree of accuracy [16]. Thermodynamic data for each species is predicted by group additivity (GA) when it is not provided by a thermodynamic library. The core expansion process is then repeated with the new enlarged core, until the predefined termination criteria are met. Kinetic and thermodynamic data may also be provided in the form of seed mechanisms and thermodynamic libraries.

The ethyl and butyl mechanisms were seeded with literature sourced sub-mechanisms for DEE [19], ethanol [20], DNBE [21], and n-butanol [22]. When available, pressure dependent rates are included from seed mechanisms and RMG libraries, in the format they are presented in their respective sources. Sub-mechanisms for EL and nBL were produced based on literature sourced rates for appropriate esters, ketones, ethers, and alkanes, as detailed in Supplementary Materials (SM). A small molecule core was provided based on the widely validated AramcoMech 2.0 [23]. Thermodynamic data are obtained from the pre-existing RMG libraries and seed mechanisms where appropriate (as identified by pre-modification annotated mechanisms, provided in SM). Otherwise, values are derived via GA. To minimise parameter error in the estimation of reaction rates relevant to the oxidation of these biofuel species, modifications were made to RMG's open-source database. This is necessary for the accurate prediction of many oxygenated compounds, as training data for the associated functional groups is not comprehensive. Database modifications such as these can have significant impacts on the predictive capabilities of RMG mechanisms, as shown in Fig. 1. In this study, an additional 470 training reactions and 43 structural groups were included in the underlying database (available in SM), with the majority sourced from the literature, and a small amount provided by CBS-QB3 [24] level calculations available in the RMG GitHub repository [12]. Mechanisms were generated using the simpleReactor module, for T = 500–1500 K, P = 1–40 bar, and φ=1.0.

After generation was complete, each mechanism was subject to a suite of post-processing techniques. This included local [OH] and brute force ΔH_f,298 K sensitivity analysis (SA). Sensitive reactions and species identified for further investigation were updated with high-quality contemporary rate parameters and thermodynamic data from literature sources where available, focussing on the minimisation of parameter uncertainties. Data was selected hierarchically, with experimental measurements and relatively low uncertainty calculations being preferred. A similar ranking is method is utilised in the RMG database. For the ethyl blend mechanism, modifications of note include the updating of rate parameters for H-abstractions of levulinic acid by HO_2 radical. These were identified as sensitive by local [OH] SA and rates

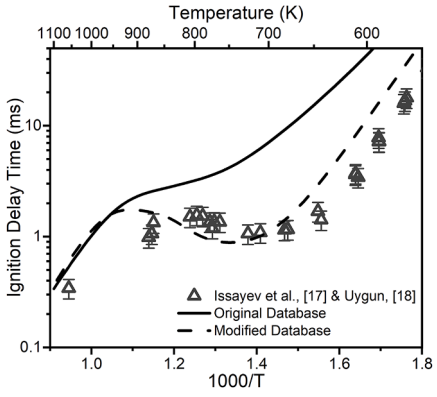

Fig. 1. Example constant volume simulations showing the impact of database modifications on the prediction of IDTs of diethyl ether (DEE). Symbols: experimental data [17,18]. Stoichiometric, P_c = 20 bar.

were replaced with appropriate analogies to ester and ketone species [25,26]. In the case of the butyl blend mechanism, H-abstractions for n-butanol by HO_2 (also identified as sensitive in [22]) were updated to match CBS-QB3 level calculations of Moc et al. [27]. H-abstractions of DNBE by HO_2 were modified to correct an error in the original mechanism, which incorrectly applied the "per H atom" rates of Mendes et al. [28] without accounting for the number of H atoms at each site (as done by Zhong and Han [21]).

The mechanism generation process has been briefly summarised in this section for the convenience of the reader. For a comprehensive description of this methodology and analysis of the impacts of these modifications on the predictive qualities of an automatically generated mechanism, the reader is directed to the study of Michelbach and Tomlin [12].

Using this process, an ethyl blend mechanism was produced which contains 595 species and 12,905 reactions, and a butyl blend mechanism was generated containing 1007 species and 21,952 reactions. The newly generated mechanisms used in this study are provided in SM, as are the newly produced seed mechanisms and full lists of post-processing-based mechanism modifications.

2.2. Model simulations

IDT simulations were performed using the closed homogeneous gas-phase reactor module available in CHEMKIN-PRO [29]. Variable volume simulations were performed by applying case dependant volume histories to account for RCM facility effects.

Speciation predictions are compared against literature data from jet stirred reactors (JSRs). Simulations for JSR data were completed using the perfectly stirred reactor module of CHEMKIN-PRO, using an isothermal, constant pressure approach.

2.3. Experimental methodology

New experimental data were collected for the IDTs of two ethyl and two butyl blends, which have not previously featured in the literature, for stoichiometric conditions, P_c=20 bar, and T_c=645–960 K. Both sets of blends contain one mixture which is designed to meet a predicted RON of 95, using a linear blending relationship (termed ELV1 and BLV1), and another mixture chosen to be within previously defined blending limits [30] (termed ELV2 and BLV2). The mole fractions for each component of these blends are given in Table 1. Due to the low vapour pressure of nBL, butyl blends were diluted to a total fuel mole fraction of 1 %. Precise mole fractions for the fuel/diluent mixtures are provided in SM, alongside tabulated measurements, and RCM volume histories.

IDTs were measured in the KAUST RCM. A detailed overview of the facility can be found in previous studies [17,31], with a brief introduction provided here. The KAUST RCM features a twin-opposed piston design, ensuring faster compression times and reduced vibrations. The combustion chamber bore is 2 inches, and the compression ratio can be varied up to 16.8. Creviced pistons are driven pneumatically, and a hydraulic locking system is used to stop and lock them at the end of compression (EOC). The combustion chamber pressure signals were recorded using a flush mounted Kistler 6045B pressure transducer. A total of 500 ms test time was recorded at 1 MHz sampling frequency for each test reported herein.

Table 1
Mole fractions for each component in ethyl and butyl blends.

Blend	Alkyl Levulinate	Di-alkyl Ether	Alcohol
ELV1	0.544	0.107	0.349
ELV2	0.657	0.237	0.106
BLV1	0.597	0.053	0.350
BLV2	0.711	0.197	0.092

Mixtures were prepared at least 1 hour prior to the experiments in two magnetically stirred 20 L heated (120 °C) mixing tanks. MKS pressure transducers (100 and 10,000 Torr) with accuracies of 0.5 % from the reading were used to measure the pressures for mixture preparation. Three different diluents (CO_2, N_2 and Ar) in various ratios were used. Due to the low vapour pressure of the fuels, the combustion chamber was heated to a range of 90–140 °C to vary EOC temperatures. Utmost care was taken during the experiments: the combustion chamber and piston heads were cleaned, and the seals were changed after each heating cycle to ensure the repeatability of the data. The estimated uncertainties for IDT measurements are in the range of 15–20 % for the liquid fuels used in this study. A representative pressure profile from KAUST RCM is shown in SM. IDT was determined as the time interval between the EOC and point of maximum dP/dt.

3. Mechanism performance

In this section, the generated ethyl and butyl mechanisms are evaluated against IDTs and JSR speciation data for individual fuel components and several ternary fuel blends. This includes the new experimental measurements collected as part of this study, as well as various literature datasets. Predictions for DEE and DEE/ethanol blends are not presented in this article, as they are functionally identical to those shown in the authors' previous work, due to the adoption of the same mechanism generation methodology [12]. These predictions are included in SM.

3.1. Ethanol

The Arrhenius autoignition behaviour of ethanol is well documented in the literature [32]. In this section, the ethanol IDT predictions of the ethyl blend mechanism are evaluated against the RCM IDT measurements of Zyada and Samimi-Abianeh [14]. RCM volume histories are not provided in their study, instead heat loss is accounted for through the use of an effective pressure, as suggested by the authors [14]. The predictive capabilities of the mechanism can be seen for various equivalence ratios (φ=0.5, 1.0, and 2.0) in Fig. 2. A figure showing the effect of pressure (P_c=15 and 30 bar) is provided in SM. Throughout all these conditions, the mechanism produces highly accurate predictions (a tabulated quantitative comparison between literature sourced data and model predictions is provided in SM). At the highest temperatures for each mixture, diluent fractions are changed to match those reported from experiments, producing a shift to slightly longer IDTs.

3.2. Ethyl levulinate

The availability of fundamental combustion data for EL is limited,

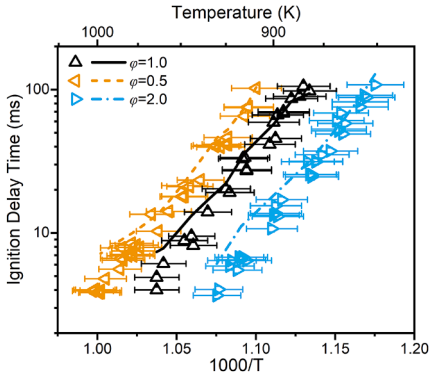

Fig. 2. Ethanol IDTs at P_c=15 bar. Symbols: experimental data [14]; lines: model predictions. Error bars represent the uncertainty in compressed gas temperatures and IDTs [14].

and low temperature IDT measurements do not currently exist. This is likely due to the molecule's low vapour pressure (0.17 mbar at 298 K), which makes gas-phase experiments incredibly difficult. However, Ghosh et al. [33] utilised a heavily diluted EL (0.5 % by mole) mixture to measure shock tube (ST) IDTs for stoichiometric and lean (φ=0.5) mixtures. The experimental results of Ghosh et al. [33] and the predictions of the RMG mechanism can be seen in Fig. 3. Predictions are again extremely accurate. However, these IDT measurements all occur at high temperatures (>1100 K) and therefore do not reveal much information about the low temperature behaviour of interest for conventional engine technologies.

Some information about the low temperature oxidation of EL can be determined from the JSR speciation data shown in Fig. 4. Mole fraction measurements here are reproduced from the work of Wang [34]. At these conditions, EL displays no notable NTC behaviour. This is predicted by the mechanism, as are the mole fractions for C_2H_4, which serve as a convenient marker for assessing the unimolecular decomposition of EL into levulinic acid. The accuracy of predictions for this speciation data provides a degree of confidence in the reproduction of EL's low temperature behaviour.

3.3. Ternary ethyl blends

In this work, we measured IDTs of ELV1 and ELV2 blends in the rapid compression machine at stoichiometric conditions and P_c=20 bar. Additionally, literature IDT measurements of an ethyl blend, as reported by Howard et al. [7] for 35/27/38 mol% EL/DEE/ethanol (EG), are included in Fig. 5. When viewing the experimental data, it is apparent that each of the investigated ethyl blends displays behaviour indicative of competing low-temperature oxidation pathways. In the cases of ELV2 and EG, this is present as distinct NTC regions. The response of IDTs to blending, highlights the influence of the ether fraction, an increase of which produces a decrease in IDTs. This is in agreement with the findings of Howard et al. [4], with respect to DCN and RON. This trend is replicated well by the ethyl blend mechanism, which provides reasonably accurate IDT predictions for each of the blends, particularly ELV2. This demonstrates the capabilities of the AMG generated mechanism and the generation methodology applied in this study for predicting the combustion behaviour of potential advanced biofuel blends. However, for both ELV1 and EG, the intensity of the experimentally observed NTC behaviour (or NTC-like behaviour for ELV1) is not as accurately predicted. Further work may be required to improve the mechanism in these areas, but it is likely to be reliant on fundamental experimental data and mathematically derived thermochemical values of relevance to ethyl levulinate oxidation (something which is sparse in the literature).

Local [OH] sensitivity analyses performed for each blend (results provided in SM) indicate that, at 750 K, reactivity is primarily driven by hydrogen abstraction (H-abstraction) reactions. The abstractions from

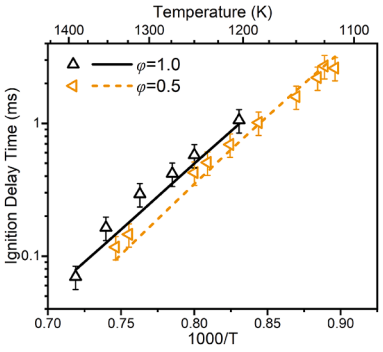

Fig. 3. IDTs for highly diluted (0.5% mol) EL mixtures at 10 bar [33]. Symbols: experimental data; lines: model predictions. Errors represent a ± 15 % uncertainty in IDTs.

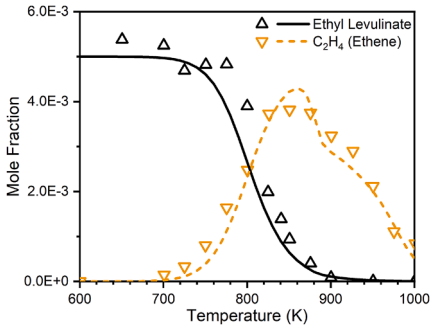

Fig. 4. EL conversion and C_2H_4 production as a function of T. Stoichiometric, 0.5% mol EL, 1 bar, 2 s residence time. Symbols: data from [34]; lines: model predictions.

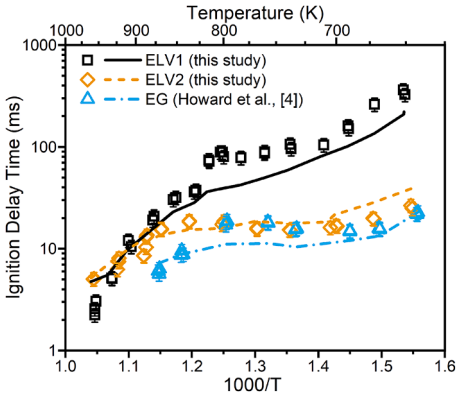

Fig. 5. IDTs for various ethyl blends at φ=1.0 and P_c=20 bar. Symbols: experimental data; squares: this work; triangles: literature data [4]. Lines: ethyl model predictions.

DEE by OH and HO_2 radicals to form the secondary fuel radical ($C_2H_5OC_2H_4$-A) are important in all cases for promoting reactivity. This is true even for the ELV1 blend, which only contains ~11 % DEE (by mole). For the blends with larger fractions of ethanol (ELV1 and EG), H-abstractions of ethanol by OH have the opposite effect, decreasing reactivity. However, it is not until temperatures of ~ 900 K that the influence of EL (ethyl levulinate) H-abstractions becomes significant. At this temperature, H-abstractions from DEE by OH also become less significant, with abstractions by HO_2 for all fuel species becoming more important for promoting reactivity. As is expected, the decomposition of H_2O_2 to produce two OH radicals becomes dominant at such temperatures.

3.4. Di-n-Butyl ether

DNBE IDTs for the temperature region of interest (~700–1000 K) appear to be absent from the literature. However, the chemical kinetic study of Thion et al. [35] provides mole fraction measurements for DNBE conversion in a JSR, which encompass the temperature region of interest at a relevant pressure and equivalence ratio. This provides some insight into the low-temperature behaviour of DNBE, including the two NTC regions. While the model does not predict the intensity of the first NTC region, the NTC observed at 700–800 K is well predicted by the model, as shown in Fig. 6.

3.5. n-Butanol

Stoichiometric ST IDTs of n-butanol for P_c=10, 20, and 40 bar are reproduced from the work of Heufer et al. [36] and shown in Fig. 7. The combined butyl mechanism provides excellent predictions for these

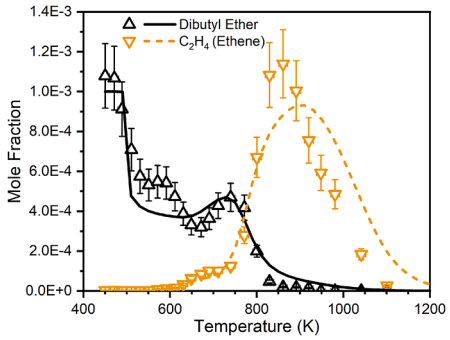

Fig. 6. DNBE conversion and C_2H_4 production in a JSR. 0.1% mol DNBE, φ=1.0, 10 atm, 0.7 s residence time. Symbols: data from [35]; lines: model predictions. Errors represent a measurement uncertainty of ±15 % [35].

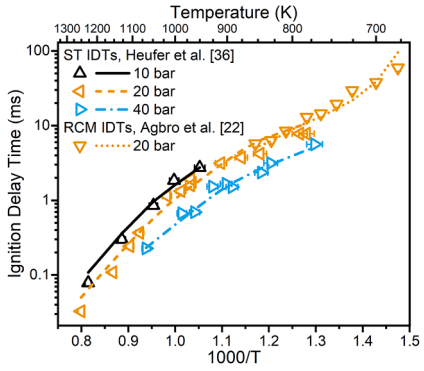

Fig. 7. Stoichiometric IDTs for n-butanol. Symbols: experimental data [22,36]; lines: model predictions.

measurements at all investigated pressures. The influence of pressure on the autoignition of n-butanol is well represented by the butyl blend mechanism, with little room for improvement. At lower temperatures, the model continues to provide accurate predictions for the RCM IDTs of Agbro et al. [22].

3.6. *Ternary butyl blends*

Measurements for butyl blend IDTs (Fig. 8) do not display the same low temperature behaviour exhibited for ethyl blends, despite the similar blend formulation methodologies. This is a result of the necessary dilution of the butyl fuel components, due to the very low vapour pressure of nBL. Experimental results may give the impression of some

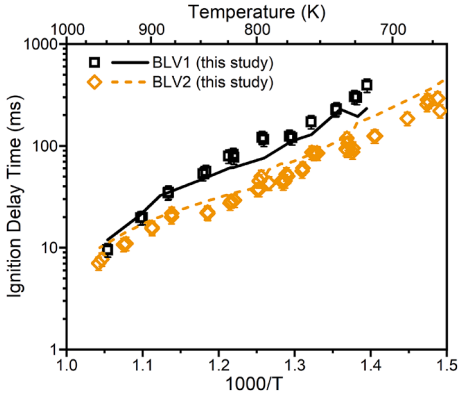

Fig. 8. IDTs for butyl blends at φ=1.0 and P_c=20 bar. Symbols: experimental data (this work); lines: model predictions; BLV1 (black), BLV2 (orange).

low temperature behaviour at the conditions 775–800 K for BLV1 and 850–875 K for BLV2. At these conditions, the rate at which reactivity increases with increasing temperature is temporarily reduced. However, in each case, this change coincides with a change in the diluent composition. Given the influence of diluent gases on RCM IDTs [37], and the large total diluent fraction, it would be inappropriate to attribute these areas to complex low temperature oxidation chemistry without additional experimental data. Considering the lack of available literature data for the butyl components (particularly nBL), the performance of the model is very promising, highlighting the capabilities of the mechanism generation methodology. The balance between the ether fraction and combined alcohol and levulinate fractions appears to determine IDTs, (as was also the case for ethyl blends) and this trend is predicted by the model.

Like the ethyl blends, the reactivity of the butyl blends at 750 K is dictated by site-specific H-abstractions (local [OH] sensitivity analysis results provided in SM). However, in the butyl case, it is H-abstractions of nBL by OH which are the most influential. Abstractions from the site adjacent to the ketone moiety, to form the secondary radical $C_9H_{15}O_3$(2), inhibit reactivity, while abstractions from the alkane chain portion of nBL to form $C_9H_{15}O_3$(5) increase reactivity. The consequences of these abstractions can be seen in Fig. 9, which presents reaction flux analysis for selected nBL reaction pathways at the same reactor conditions as the sensitivity analysis. These conditions provide a good correlation between IDTs and RON [38], and are similar to those previously explored in the investigation of EG [4,7]. By exploring pathways at a time of 67 % IDT, the evolving and complex low-temperature chemistry can be investigated. Reaction pathways with the highest flux are presented alongside selected high-sensitivity reactions. Similar analyses of n-butanol and DNBE are present in the literature and are not repeated here [32,35]. The major pathways for the further reactions of $C_9H_{15}O_3$(2) are chain terminating, whereas $C_9H_{15}O_3$(5) follows a typical oxidation and internal isomerisation pathway, which will ultimately increase reactivity through the generation of multiple radicals (this pathway is shown up to the relative O_2QOOH species for conciseness). The internal isomerisation of $C_9H_{15}O_5$(3) to $C_9H_{15}O_5$(19) is important for driving this pathway forward, as indicated by sensitivity analysis results. This is in competition with HO_2 eliminations from both species, which are all sensitive and decrease reactivity, generating unreactive alkenyl levulinates.

Interestingly, at these conditions nBL reaction pathways display significant differences for BLV1 and BLV2. In particular, reactions with O_2 show a much lower flux throughout the regime for BLV2. This is a result of multi-stage ignition, which is present in BLV2 simulations but not BLV1 due to the larger fraction of DNBE [31]. The 1st stage ignition increases the temperature and pressure within the reactor, causing a relative increase in the rate of chain terminating reactions for nBL indicative of NTC behaviour. A shift towards scission reactions can also be seen in changes to the radical pool (Fig. 10). BLV2 shows a relative increase in CH_3 radical production, which coincides with a substantial decrease in the relative flux of $C_9H_{15}O_3$(5) oxidation and an increase in the competing scission, producing an unreactive $C_8H_{12}O_3$ (allyl levulinate) and a CH_3 radical.

At 900 K, abstractions from nBL are not as influential. Instead, H-abstractions from DBE and n-butanol by HO_2 become important, as does the decomposition of nBL to produce levulinic acid and 1-butene. H-abstractions of fuel species by HO_2 are more influential at these intermediate temperatures (i.e., ~800–900 K), as discussed previously [39].

4. Conclusions

AMG tools have proven to be effective at producing accurate models for complex oxygenated fuels when applied appropriately. The method employed in this study, utilised database additions and modifications based on low uncertainty, high quality, literature data and various post-processing steps. The resulting mechanisms were shown to produce

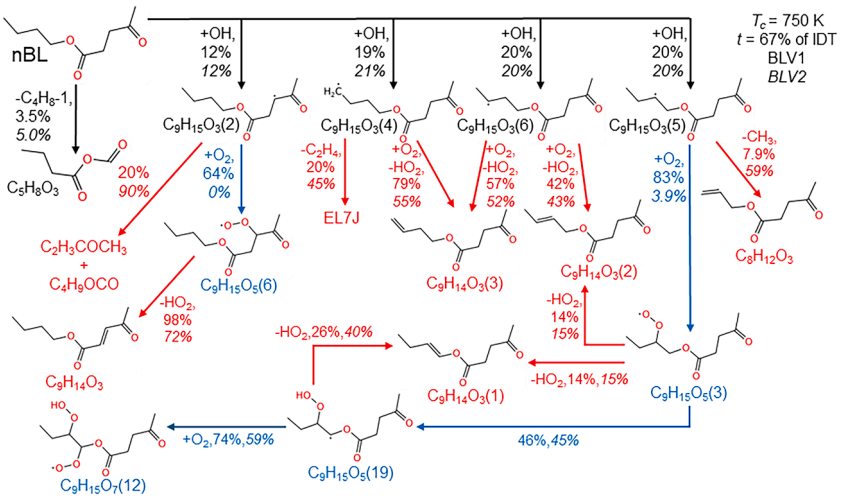

Fig. 9. Reaction flux analysis at 67 % of IDT, T_c=750 K, φ=1.0, and P_c=20 bar. Fuel radical consumption pathways are calculated after considering the change in concentrations following isomerisation reactions. Blue: chain propagating or branching. Red: chain terminating.

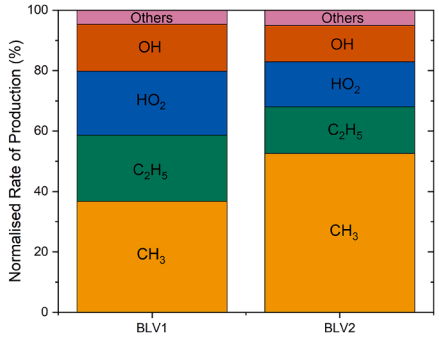

Fig. 10. Normalised small radical rate of production for butyl blends at 2/3rd IDT, T_c=750 K, φ=1.0, and P_c=20 bar.

highly accurate predictions for a range of target parameters for both component species and fuel blends. The mechanisms may also be extrapolated outside the regime of their seed mechanisms, as highlighted by predictive capabilities of the mechanisms when evaluated for ternary ethyl and butyl fuel blends.

For the first time, ignition data for butyl blends featuring the products of biomass butanolysis have been presented, alongside the data for new ethyl blends. The suite of blends presented are all of relevance to modern engines, and predictions for ethyl blends show that these advanced biofuel blends are capable of replicating the ignition behaviour typical of modern gasoline blends [7]. Similar behaviour was not observed in the RCM for the butyl blends, likely due to the need for dilution, which suppresses NTC behaviour. The AMG produced mechanisms were able to capture the experimentally determined blending behaviour and provide some evidence for NTC-driving low temperature reaction pathways in butyl blends. However, additional experimental work (i.e., RCM IDTs or JSR measurements) is required to confidently state that nBL produces an NTC region.

Novelty and significance statement

The work presents the evaluation of complex mechanisms for blends of oxygenated advanced biofuel components produced using automatic mechanism generation (AMG) techniques. The application of AMG tools for oxygenated species is extremely rare in the literature, partly due to the lack of availability of supporting databases. The current work provides a successful case study of its application to example biofuel blends, as well as data resources in supplementary materials that will assist future researchers in building mechanisms for other oxygenates. As the EU mandates increasing fractions of advanced biofuels within transport fuels, the availability of such methodological protocols and supporting data is extremely timely. The mechanisms are shown to accurately predict the blending behavior of potentially tailorable advanced biofuel blends from alcoholysis of lignocellulosic biomass feedstocks. The resulting models can be used to evaluate the combustion performance of various blend ratios, allowing optimization of engine performance and emissions characteristics.

Author contributions

CM: Performed research (computational), paper writing.
AT: Project lead, paper writing.
KH: Performed research (experimental), paper writing.
AF: Supervision (KH), paper editing.

Declaration of competing interest

The authors declare that they have no known competing financial interests or personal relationships that could have appeared to influence the work reported in this paper.

Acknowledgements

This research was funded by the EPSRC grant EP/T033088/1. The authors would like to thank all members of the SusLABB (Sustainable Low Cost Lignocellulosic Advanced Biofuel Blends) group for their input and support. The work of KAUST authors was funded by an internal research grant of King Abdullah University of Science and Technology.

Supplementary materials

Supplementary material associated with this article can be found, in the online version, at doi:10.1016/j.proci.2024.105667.

References

[1] IEA (2022), World Energy Outlook 2022, Paris, 2022. https://www.iea.org/reports/world-energy-outlook-2022.
[2] European Commission, Directive (EU) 2018/2001 of the european parliament and of the council - of 11 december 2018 - on the promotion of the use of energy from renewable sources, Off. J. Eur. Union (2018) 128.
[3] J.F. LealSilva, R. Grekin, A.P. Mariano, R. MacielFilho, Making levulinic acid and ethyl levulinate economically viable: a worldwide technoeconomic and

environmental assessment of possible routes, Energy Technol 6 (2018) 613–639, https://doi.org/10.1002/ente.201700594.
[4] M.S. Howard, G. Issayev, N. Naser, S.M. Sarathy, A. Farooq, S. Dooley, Ethanolic gasoline, a lignocellulosic advanced biofuel, Sustain. Energy Fuels 3 (2019) 409–421, https://doi.org/10.1039/C8SE00378E.
[5] J.R. Melendez, B. Mátyás, S. Hena, D.A. Lowy, A. El Salous, Perspectives in the production of bioethanol: a review of sustainable methods, technologies, and bioprocesses, Renew. Sustain. Energy Rev 160 (2022) 112260, https://doi.org/10.1016/j.rser.2022.112260.
[6] Y. Liu, Y. Yuan, G. Ramya, S. Mohan Singh, N. Thuy Lan Chi, A. Pugazhendhi, C. Xia, T. Mathimani, A review on the promising fuel of the future – Biobutanol; the hindrances and future perspectives, Fuel 327 (2022) 125166, https://doi.org/10.1016/j.fuel.2022.125166.
[7] M.S. Howard, G. Issayev, N. Naser, S.M. Sarathy, A. Farooq, S. Dooley, Correction: ethanolic gasoline, a lignocellulosic advanced biofuel, Sustain. Energy Fuels 6 (2022) 3080–3083, https://doi.org/10.1039/D2SE90024F.
[8] A.M.R. Galletti, G. Caposciutti, G. Pasini, M. Antonelli, S. Frigo, Bio-additives for CI engines from one-pot alcoholysis reaction of lignocellulosic biomass: an experimental activity, E3S Web Conf. 197 (2020) 08005, https://doi.org/10.1051/e3sconf/202019708005.
[9] L.J. Broadbelt, J. Pfaendtner, Lexicography of kinetic modeling of complex reaction networks, AIChe J. 51 (2005) 2112–2121, https://doi.org/10.1002/aic.10599.
[10] S. Brunialti, X. Zhang, T. Faravelli, A. Frassoldati, S.M. Sarathy, Automatically generated detailed and lumped reaction mechanisms for low- and high-temperature oxidation of alkanes, Proc. Combust. Inst. 39 (2023) 335–344, https://doi.org/10.1016/j.proci.2022.08.084.
[11] M.S. Johnson, M.R. Nimlos, E. Ninnemann, A. Laich, G.M. Fioroni, D. Kang, L. Bu, D. Ranasinghe, S. Khanniche, S.S. Goldsborough, S.S. Vasu, W.H. Green, Oxidation and pyrolysis of methyl propyl ether, Int. J. Chem. Kinet. 53 (2021) 915–938, https://doi.org/10.1002/kin.21489.
[12] C.A. Michelbach, A.S. Tomlin, Automatic mechanism generation for the combustion of advanced biofuels: a case study for diethyl ether, Int. J. Chem. Kinet. 56 (2024) 233–262, https://doi.org/10.1002/kin.21705.
[13] M. Liu, A. Grinberg Dana, M. Johnson, M. Goldman, A. Jocher, A.M. Payne, C. Grambow, K. Han, N.WW. Yee, E. Mazeau, K. Blondal, R. West, F. Goldsmith, W.H. Green, Reaction mechanism generator v3.0: advances in automatic mechanism generation, (2020). https://doi.org/10.26434/chemrxiv.13489656.v1.
[14] A. Zyada, O. Samimi-Abianeh, Ethanol kinetic model development and validation at wide ranges of mixture temperatures, pressures, and equivalence ratios, Energy Fuels. 33 (2019) 7791–7804, https://doi.org/10.1021/acs.energyfuels.9b01035.
[15] R.G. Susnow, A.M. Dean, W.H. Green, P. Peczak, L.J. Broadbelt, Rate-based construction of kinetic models for complex systems, J. Phys. Chem. A 101 (1997) 3731–3740, https://doi.org/10.1021/jp9637690.
[16] C.W. Gao, J.W. Allen, W.H. Green, R.H. West, Reaction Mechanism Generator: automatic construction of chemical kinetic mechanisms, Comput. Phys. Commun. 203 (2016) 212–225, https://doi.org/10.1016/j.cpc.2016.02.013.
[17] G. Issayev, S. Mani Sarathy, A. Farooq, Autoignition of diethyl ether and a diethyl ether/ethanol blend, Fuel 279 (2020) 118553, https://doi.org/10.1016/j.fuel.2020.118553.
[18] Y. Uygun, Ignition studies of undiluted diethyl ether in a high-pressure shock tube, Combust. Flame 194 (2018) 396–409, https://doi.org/10.1016/j.combustflame.2018.05.022.
[19] L.-S. Tran, O. Herbinet, Y. Li, J. Wullenkord, M. Zeng, E. Bräuer, F. Qi, K. Kohse-Höinghaus, F. Battin-Leclerc, Low-temperature gas-phase oxidation of diethyl ether: fuel reactivity and fuel-specific products, Proc. Combust. Inst. 37 (2019) 511–519, https://doi.org/10.1016/j.proci.2018.05.135.
[20] Y. Zhang, H. El-Merhubi, B. Lefort, L. Le Moyne, H.J. Curran, A. Kéromnès, Probing the low-temperature chemistry of ethanol via the addition of dimethyl ether, Combust. Flame 190 (2018) 74–86, https://doi.org/10.1016/j.combustflame.2017.11.011.
[21] A. Zhong, D. Han, Experimental and kinetic modelling studies on di-n-butyl ether (DBE) low temperature auto-ignition, Combust. Flame 237 (2022) 111882, https://doi.org/10.1016/j.combustflame.2021.111882.
[22] E. Agbro, A.S. Tomlin, M. Lawes, S. Park, S.M. Sarathy, The influence of n-butanol blending on the ignition delay times of gasoline and its surrogate at high pressures, Fuel 187 (2017) 211–219, https://doi.org/10.1016/j.fuel.2016.09.052.
[23] Y. Li, C.-W. Zhou, K.P. Somers, K. Zhang, H.J. Curran, The oxidation of 2-butene: a high pressure ignition delay, kinetic modeling study and reactivity comparison with isobutene and 1-butene, Proc. Combust. Inst. 36 (2017) 403–411, https://doi.org/10.1016/j.proci.2016.05.052.
[24] J.A. Montgomery Jr., M.J. Frisch, J.W. Ochterski, G.A. Petersson, A complete basis set model chemistry. VII. use of the minimum population localization method, J. Chem. Phys. 112 (2000) 6532–6542, https://doi.org/10.1063/1.481224.
[25] J. Mendes, C.-W. Zhou, H.J. Curran, Theoretical and kinetic study of the hydrogen atom abstraction reactions of esters with HȮ2 radicals, J. Phys. Chem. A 117 (2013) 14006–14018, https://doi.org/10.1021/jp409133x.
[26] S. Thion, P. Diévart, P. Van Cauwenberghe, G. Dayma, Z. Serinyel, P. Dagaut, An experimental study in a jet-stirred reactor and a comprehensive kinetic mechanism for the oxidation of methyl ethyl ketone, Proc. Combust. Inst. 36 (2017) 459–467, https://doi.org/10.1016/j.proci.2016.05.022.
[27] J. Moc, G. Black, J.M. Simmie, H.J. Curran, The unimolecular decomposition and H abstraction reactions by HO and HO2 from n-butanol, AIP Conf. Proc. 1148 (2009) 161–164, https://doi.org/10.1063/1.3225261.
[28] J. Mendes, C.-W. Zhou, H.J. Curran, Rate constant calculations of h-atom abstraction reactions from ethers by HȮ2 radicals, J. Phys. Chem. A 118 (2014) 1300–1308, https://doi.org/10.1021/jp412496g.
[29] Reaction Design, CHEMKIN-PRO 15112, Reaction design, San Diego, 2011.
[30] S. Wiseman, C.A. Michelbach, H. Li, A.S. Tomlin, Predicting the physical properties of three-component lignocellulose derived advanced biofuel blends using a design of experiments approach, Sustain. Energy Fuels 7 (2023) 5283–5300, https://doi.org/10.1039/D3SE00822C.
[31] K. Hakimov, F. Arafin, K. Aljohani, K. Djebbi, E. Ninnemann, S.S. Vasu, A. Farooq, Ignition delay time and speciation of dibutyl ether at high pressures, Combust. Flame 223 (2021) 98–109, https://doi.org/10.1016/j.combustflame.2020.09.028.
[32] S.M. Sarathy, P. Oßwald, N. Hansen, K. Kohse-Höinghaus, Alcohol combustion chemistry, Prog. Energy Combust. Sci. 44 (2014) 40–102, https://doi.org/10.1016/j.pecs.2014.04.003.
[33] M.K. Ghosh, M.S. Howard, Y. Zhang, K. Djebbi, G. Capriolo, A. Farooq, H.J. Curran, S. Dooley, The combustion kinetics of the lignocellulosic biofuel, ethyl levulinate, Combust. Flame 193 (2018) 157–169, https://doi.org/10.1016/j.combustflame.2018.02.028.
[34] J.-Y. Wang, Experimental and kinetic modeling study of ethyl levulinate oxidation in a jet-stirred reactor, Thesis (2017), https://doi.org/10.25781/KAUST-6G3BM.
[35] S. Thion, C. Togbé, Z. Serinyel, G. Dayma, P. Dagaut, A chemical kinetic study of the oxidation of dibutyl-ether in a jet-stirred reactor, Combust. Flame 185 (2017) 4–15, https://doi.org/10.1016/j.combustflame.2017.06.019.
[36] K.A. Heufer, R.X. Fernandes, H. Olivier, J. Beeckmann, O. Röhl, N. Peters, Shock tube investigations of ignition delays of n-butanol at elevated pressures between 770 and 1250K, Proc. Combust. Inst. 33 (2011) 359–366, https://doi.org/10.1016/j.proci.2010.06.052.
[37] S.W. Wagnon, M.S. Wooldridge, Effects of buffer gas composition on autoignition, Combust. Flame 161 (2014) 898–907, https://doi.org/10.1016/j.combustflame.2013.09.022.
[38] E. Singh, J. Badra, M. Mehl, S.M. Sarathy, Chemical kinetic insights into the octane number and octane sensitivity of gasoline surrogate mixtures, Energy Fuels. 31 (2017) 1945–1960, https://doi.org/10.1021/acs.energyfuels.6b02659.
[39] C. Michelbach, A. Tomlin, An experimental and kinetic modeling study of the ignition delay and heat release characteristics of a five component gasoline surrogate and its blends with iso-butanol within a rapid compression machine, Int. J. Chem. Kinet. 53 (2021) 787–808, https://doi.org/10.1002/kin.21483.